CSAWAC 43 (4) 463-620 (2015) · Vol. 43 · No. 4 · April 2015

CLEAN

Soil Air Water

Renewables

Sustainability

Environmental Monitoring

4 | 2015

www.clean-journal.com

WILEY

CLEAN
Soil Air Water

Anisa Ur Rahmah
Sabtanti Harimurti
Abdul Aziz Omar
Thanapalan Murugesan

Department of Chemical Engineering, Universiti Teknologi PETRONAS, Bandar Seri Iskandar, Tronoh, Perak, Malaysia

Research Article

Kinetics and Thermodynamic Studies of Oxytetracycline Mineralization Using UV/H_2O_2

Oxytetracycline (OTC), a widely used antibiotic, was taken as the model contaminant to study the kinetic and thermodynamic parameters of mineralization using a UV/H_2O_2 system. Mineralization experiments were carried out at different initial OTC concentrations of 0.0156–0.0531 M, initial H_2O_2 concentrations of 0.043–0.116 M and at a temperature range of $20-50\,^{\circ}C$. The OTC mineralization process was monitored by measuring the total organic carbon as well as H_2O_2 consumption. The analysis of mineralization data showed two phases of mineralization: phase I: $0 \le t \le 30$ min and phase II: $30 \le t \le 180$ min. Based on this, the kinetic and thermodynamic parameters were established. The order of reaction obtained for organic C and H_2O_2 is 0.624 and 0.599 (phase I) and 0.954 and 0.062 (phase II), respectively. Based on this kinetic model, the OTC degradation rate constants were 0.0069 min^{-1} (phase I) and 0.0051 min^{-1} (phase II). The activation energy for phase I and phase II oxidation was 10.236 and 9.913 kJ mol^{-1}, respectively. The estimated $\Delta^{\#}G$ and $\Delta^{\#}H$ values are positive, whereas negative $\Delta^{\#}S$ values were obtained.

Keywords: Antibiotics; Degradation; Oxidation processes; Personal care products; Pharmaceuticals

Received: December 25, 2012; *revised:* July 30, 2013; *accepted:* November 14, 2013

DOI: 10.1002/clen.201200637

1 Introduction

Pharmaceutical and personal care products (PCPs) are extensively used in our modern living, such as prescribed therapeutic drugs, veterinary drugs, cosmetics, and fragrances or even nutraceutical products (i.e. vitamin and hormones, etc.) [1]. In general they are used for improving the quality of personal health and growth of human and other organism or for cosmetic reasons [1, 2]. Residues of PCPs may come from pharmaceutical industries, hospital and households, veterinary drug (mainly antibiotics and steroids) and agricultural sectors, etc. [3–6]. Among the PCPs, antibiotics are one of the important types of compounds that are produced and consumed in very large quantity to treat bacterial diseases in human and animal. Excretion of metabolized and non-metabolized form of antibiotics from human and animal bodies may enter into the water stream [6]. Many researchers have reported that contamination in surface and ground water, drinking water, tap water, ocean water, sediments, and soil might be due to antibiotics [7–9]. These contaminations will produce antibiotic-resistant bacteria and damage the internal organ of aquatic animals [10–12]. Water contaminated with antibiotics, when it is consumed by the animals, they remain inside the tissues as food pollutant which might trigger the allergic reactions and contribute to the formation and development of antibiotic-resistant bacteria in human body [13].

Antibiotics are classified under several categories namely: β-lactams, tetracyclines, aminoglycosides, quinolones, macrolides, glycopeptides, and sulfonamides. However, the most extensively used antibiotics in animal feeds are tetracycline class including as food additive for systemic bacterial infection therapy in farmed fish, growth simulator in livestock and stress reduction in pig and poultry [14–17]. Hence, in the present study oxytetracycline (OTC), a member of the tetracycline class has been chosen as a model antibiotic compound that contaminates the water matrix.

Many methods have been applied to treat the antibiotic contaminated water matrix. However, antibiotics are extremely resistant compounds toward biological degradation process, hence the research have been directed towards the application of non-biological processes for their destruction, and one among them is advanced oxidation processes (AOPs) [9]. Recently, AOPs have emerged as an effective process, which is capable of transforming organic pollutant into non-toxic substances. These processes exclusively rely on the generation of hydroxyl radicals ($^{\bullet}OH$) in general or any other highly reactive species, that can attack the organic pollutant in the water matrix. After the radical attack, the organic pollutant will be subjected to a series of degradation/oxidation reaction and lead to the formation of CO_2 and H_2O as the final product.

The degradation of OTC have been achieved through many processes namely, Fenton process, ozone process, UV photolysis, UV/H_2O_2 system, simulated sunlight irradiation, photocatalytic process using TiO_2-zeolite, electrochemical oxidation, Mn-peroxidase and γ-pulse irradiation, etc. [14, 18–25]. However, no detailed study has

Correspondence: Prof. T. Murugesan, Department of Chemical Engineering, Universiti Teknologi PETRONAS, Bandar Seri Iskandar, 31750, Tronoh, Perak D. R., Malaysia
E-mail: murugesan@petronas.com.my; tmgesan_57@yahoo.com

Abbreviations: AOP, advanced oxidation process; **OTC**, oxytetracycline; **PCP**, personal care product; **TOC**, total organic carbon

been reported on the kinetics and thermodynamic parameters of OTC mineralization using the combined UV/H_2O_2 system, especially based on total organic carbon (TOC) concentration profile. This TOC concentration profile is important since it refers to the complete conversion of organic content of compound to inorganic constituent which generally lead to complete detoxification [26]. Based on that, in the present study it is proposed to establish the details of kinetics (order of reaction, rate constant (k), energy of activation (E_A)) and thermodynamic parameters (enthalpy of activation ($\Delta^{\#}H$), Gibbs energy of activation ($\Delta^{\#}G$), and entropy of activation ($\Delta^{\#}S$)) of OTC mineralization. The evaluation and the establishment of these parameters will provide a better insight into the OTC mineralization mechanism and hence lead to their potential application toward scale up and commercialization of the process.

2 Materials and methods

2.1 Materials

OTC hydrochloride, $C_{22}H_{24}N_2O_9 \cdot HCl$ (Merck, Germany) and hydrogen peroxide, 30% (Merck, Germany) were used as the source of organic contaminant and the source of hydroxyl radical, respectively. H_2SO_4, 98% (Merck, Germany) and NaOH (Merck, Germany) were used for pH adjustment. All chemicals were used without further purification. The chemical structure of OTC is given in Fig. 1.

2.2 Methods

All experiments were carried out in a glass reactor (400 mL working volume) with a provision for irradiation using a low pressure Hg lamp (8 W power GPH295T5L; serial no. EC90277, USA) to produce UV light at 254 nm. A schematic diagram of the reactor is shown in Fig. 2. During irradiation, the solution was stirred using magnetic stirrer. The temperature was maintained using water circulation through the reactor jacket. After adjusting the OTC solution to the optimum pH, desired amount of H_2O_2 were then added into the reactor. Initial concentrations of OTC and H_2O_2 as well as temperature were varied. To monitor the progress of mineralization, about 3 mL of liquid samples were drawn from the reactor at scheduled time intervals. Since the total amount of samples withdrawn were <5% of the total volume, for calculation purposes the total sample volume was neglected. About 180 min of irradiation time were applied for all of the experiments. TOC measurements were carried out using a TOC analyzer (Shimadzu, Japan) while the amount of H_2O_2 in the solution was analyzed by colorimetric method using $KMnO_4$.

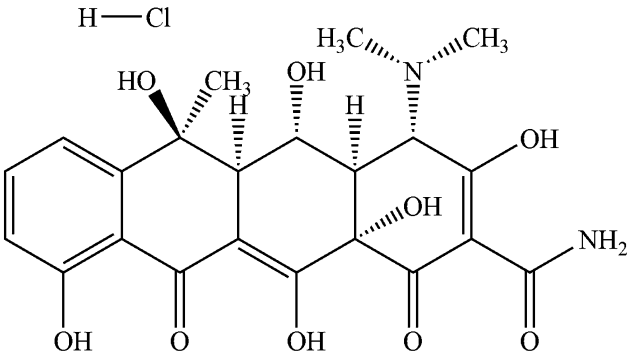

Figure 1. Chemical structure of OTC.

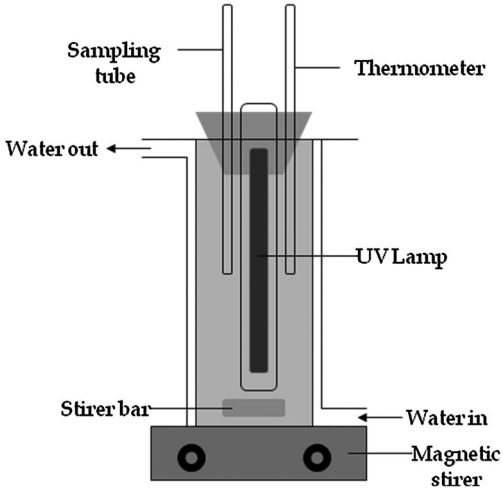

Figure 2. Schematic diagram of the UV/H_2O_2 system.

2.2.1 Theory and background

Based on the preliminary and optimization studies on OTC mineralization process using Box-Behnken experimental design combined with the response surface methodology, the optimum pH was found to be 6.36 and hence for the present experiments for the estimation of kinetic and thermodynamic parameters were conducted at pH 6.36 [27]. The measured TOC (ppm) were later converted into organic carbon concentration (org. C, M) for further analysis. Concentration of org. C and H_2O_2 in the reaction media could be directly estimated. Therefore, it is more convenient and practical to express the kinetic equation in terms of org. C and H_2O_2 concentration rather than free radical concentration. In the present study, OTC was assumed to be completely mineralized by H_2O_2 and formed inorganic products, such as H_2O, CO_2, N_2, and Cl_2 (Eq. (1)). This stoichiometric assumption was used previously to optimize the H_2O_2 mole ratio needed to completely mineralize OTC [27].

$$2C_{22}H_{24}N_2O_9 \cdot HCl + 95H_2O_2 \rightarrow 120H_2O + 44CO_2 + 2N_2 + Cl_2 \quad (1)$$

For determining the order of reaction, initial concentrations of OTC as well as H_2O_2 were varied in the range of 125–500 ppm (0.0156–0.053 M of org. C) and 0.043–0.116 M of H_2O_2, respectively. To study the individual effect of UV and H_2O_2, OTC mineralization experiments were conducted at a H_2O_2 concentration of 0.116 M only. To investigate the effect of temperature on the rate constant (k), the experiments were conducted at four different temperatures (20, 30, 40, and 50°C). The experimental data were then plotted against pseudo order, zeroth, first, and second order of kinetics. Differential method was also applied to determine the order of reaction. The activation energy (E_A) was calculated from the linearized form of Arrhenius equation, while the values of enthalpy of activation ($\Delta^{\#}H$), Gibbs energy of activation ($\Delta^{\#}G$), and entropy of activation ($\Delta^{\#}S$) were calculated by using the Eyring–Polanyi equation.

3 Results and discussion

3.1 Kinetic study

The analysis for the kinetics of mineralization was made on the assumption that the rate of reaction depend on organic C

CLEAN Soil Air Water

concentration only and hence the rate of OTC mineralization can be expressed as:

$$r = -\frac{\mathrm{d}[\text{org. C}]}{\mathrm{d}t} = k_{\text{obs}}[\text{org. C}]^{\text{n}} \quad (2)$$

Based on these assumptions, the equations for the pseudo zero-th (Eq. (3)), pseudo-first (Eq. (4)), and pseudo-second order (Eq. (5)) can be derived and expressed as follows.

$$[\text{org. C}]_0 - [\text{org. C}]_t = k_0 t \quad (3)$$

$$\ln\frac{[\text{org. C}]_t}{[\text{org. C}]_0} = -k_{\text{obs}} t \quad (4)$$

$$\frac{1}{[\text{org. C}]_t} - \frac{1}{[\text{org. C}]_0} = k_{\text{obs}} t \quad (5)$$

where n is the order of reaction, $[\text{org. C}]_0$ the initial concentration of org. C, $[\text{org. C}]_t$ the concentration of org. C at time t, k_{obs} the kinetic rate constant, and t is the time (min).

The experimental data were analyzed accordingly to the pseudo-zero-th, first, and second order of reaction, respectively. Table 1 shows the calculated kinetic rate constant along with the estimated correlation coefficients (R^2). From this table, it can be seen that the present OTC mineralization data fits well with pseudo first order kinetics with higher R^2 values (0.947–0.995) when compared to the pseudo zero-th and second order. A detailed review on the degradation and mineralization kinetics of tetracycline groups of antibiotics are summarized in Tab. 2. Based on the available literature on the degradation of tetracycline groups, namely photolysis of tetracycline hydrochloride, photolysis, and hydrolysis of OTC follow the pseudo-first order kinetics [20–25], while the ozonation and Fenton process of OTC extracted from manure sample as well as the UV/H_2O_2 process for 5 μM OTC followed the pseudo-second order kinetics [14, 25]. Even though it fits well with the first order kinetics with better R^2 value, but at the same time it yields inconsistent values for k.

The OTC mineralization was due to the $^{\bullet}$OH radical attack, which is generated from H_2O_2 dissociation by UV light rather than UV photolysis and H_2O_2 oxidation alone, as shown in Fig. 3. The measured values of the molar concentration of organic carbon with time are shown in Fig. 4. Beside the pseudo-order kinetics, the experimental data were further analyzed using differential method which includes both of org. C and H_2O_2 concentration. The differential method was applied by incorporating org. C and H_2O_2 concentrations into the kinetic equation.

$$r = \frac{-\mathrm{d}[\text{org. C}]_t}{\mathrm{d}t} = k_{\text{obs}}[\text{org. C}]^{\text{m}}[H_2O_2]^{\text{n}} \quad (6)$$

Table 1. Results of pseudo-order plots of OTC mineralization kinetics

	Pseudo zero-th order		Pseudo first order		Pseudo second order	
Org. C (M)	k	R^2	k	R^2	k	R^2
0.0156	8E−05	0.835	0.0132	0.969	3.114	0.980
0.0284	1E−04	0.932	0.0154	0.978	3.000	0.759
0.0440	8E−05	0.835	0.0112	0.995	0.759	0.892
0.0531	2E−04	0.987	0.0080	0.947	0.770	0.901

The logarithmic form of Eq. (6) was used for determining the order of reaction. By plotting the value of $\ln(\mathrm{d}[\text{org. C}]_t/\mathrm{d}t)$ vs. $\ln([\text{org. C}])$ and $\ln(\mathrm{d}[\text{org. C}]_t/\mathrm{d}t)$ vs. $\ln([H_2O_2])$, the value of the order of reaction with respect to OTC and H_2O_2 were determined, respectively. This order of reaction can be derived from negative slope of the curve. The value of the k_{obs} can be derived by introducing the estimated order of reaction into the overall kinetic equation at any OTC and H_2O_2 concentration.

A careful analysis of the plot of org. C vs. t (Fig. 4) showed two linear regions, during the time interval from 0–30 min (phase I) and 30–180 min (phase II). Plots for phase I and phase II of org. C mineralization are presented in Figs. 5 and 6, respectively, indicating a satisfactory fit of the present experimental data. The estimated overall kinetic rates for both regions are presented below.

Phase I:

$$r = 0.0069[\text{org. C}]^{0.624}[H_2O_2]^{0.599} \quad (7)$$

Phase II:

$$r = 0.0051[\text{org. C}]^{0.954}[H_2O_2]^{0.062} \quad (8)$$

By comparing all the results from R^2 and k of pseudo order (Tab. 1) and differential method plot (Tab. 3), it can be concluded that the differential method shows better representation of the data. It also provides better insight in understanding the mineralization mechanism of OTC. The total order of reaction for phases I and II are 1.223 and 1.016, respectively. Therefore, the unit of k is approximated as that for the first order of reaction, min^{-1}.

Generally, AOPs consist of two interrelated phases, i.e. generation of reactive species and oxidation of organic content which are further subdivided into series of simple oxidation and substrate mineralization [28–30]. At the earlier stage (phase I) of AOPs, the photon energy from UV lamp initiates the dissociation of H_2O_2 molecule, forming two $^{\bullet}$OH radicals. These radicals may attack the parent compound forming intermediate which are prone and unstable toward mineralization. While the latter stage (phase II) deals mostly on series of complex oxidation reactions with the reactive functional group of organic compound, C−C bond fragmentation until all C-atoms inside the organic molecule are oxidized into their highest state, i.e. CO_2, and yet having more stable structure [28].

Based on Eq. (7), both OTC and H_2O_2 molecules have a similar order of reaction. This might be due to the fact that during phase I, after dissociation of H_2O_2 molecules, the $^{\bullet}$OH radicals formed would subsequently attack the unstable parent compound of OTC which leads to the generation of intermediate compound. However, for phase II (Eq. (8)), the mineralization process predominantly depends on the org. C concentration rather than on H_2O_2 which was shown by the higher order of reaction of org. C (0.9541) compared to H_2O_2 (0.062). This could be attributed to the reason that after the disappearance of parent organic compounds, the intermediate species started to form which was further followed by the significant reduction of $^{\bullet}$OH radicals as well as H_2O_2 concentration (Fig. 7). Since OTC molecules contain N-atoms, after irradiation, beside organic acids, organic compounds containing N-atoms and intermediate compound were also detected. The parent organic compound and the intermediate compounds may compete as the contaminant target during the existing $^{\bullet}$OH radical attack. Due to these competitions, the org. C concentration predominantly affected the mineralization rates rather than H_2O_2.

Table 2. Comparison of literature on tetracycline groups degradation and mineralization kinetics

Compound	System	Kinetics	Remarks	Reference
OTC	Extracted OTC from manure sample	Pseudo-second order	434 mM H_2O_2 and 43.4 mM Fe^{2+} Ozone dose: 2.5 mg min^{-1}	[14]
	Fenton and ozonation	k_{obs}: Fenton process (119 M^{-1} s^{-1}), k_{obs}: ozonation (548 M^{-1} s^{-1})	Kinetics based on OTC concentration	
TC	Photolysis:150 W Xenon lamp	Pseudo first order k_{obs}: 0.010–0.030 min^{-1}	10 μM TC Kinetics based on OTC concentration	[20]
OTC	Photolysis:500 W Hg lamp	Pseudo first order k_{obs}: 0.0075–0.0141 min^{-1}	10–40 ppm OTC Kinetics based on OTC concentration	[21]
OTC	Hydrolysis Photolysis (sunlight irradiation)	Pseudo-first order for hydrolysis k_{obs}: 0.094 ± 0.001 until 0.106 ± 0.003 day^{-1} Pseudo-first order for photolysis k_{obs}: 3.61 ± 0.06 day^{-1}	10–230 μM of OTC Kinetics based on OTC concentration	[22]
OTC	UV only (11 W Hg lamp power) UV/H_2O_2	Pseudo-first order for direct photolysis k_{obs}: $(0.46 \pm 0.02) \times 10^3$ cm^2 mJ^{-1} (SW), $(0.50 \pm 0.03) \times 10^3$ cm^2 mJ^{-1} (DW), $(0.61 \pm 0.04) \times 10^3$ cm^2 mJ^{-1} (WW), $(1.06 \pm 0.01) \times 10^3$ cm^2 mJ^{-1} (WW) Second order for UV/H_2O_2 degradation k_{obs}: 6.96×10^9 M^{-1} s^{-1}	5 μM OTC, 1 mM H_2O_2 Different water matrix Kinetics based on OTC concentration	[25]
OTC	UV/H_2O_2 (8 W medium pressure-Hg lamp)	Two phase oxidation: Phase I: $r = 0.0069$ [org. C]$^{0.624}$ $[H_2O_2]^{0.599}$ Phase II: $r = 0.0051$ [org. C]$^{0.954}$ $[H_2O_2]^{0.062}$	125–500 ppm OTC, 0.24–0.94 mM Optimum pH at 6.3 Kinetics based on TOC value	Present study

TC, tetracycline hydrochloride, DW, treatment plant water, SW, surface water, UW, buffered water, WW, wastetwater.

Different values of k were also observed to be higher, values of phase I, compared to phase II, which indicates a higher mineralization rate. This could be attributed that at phase I higher concentrations of OTC parent compounds were present in the solution compared to more stable organic products, and hence, increased the mineralization rate. At the end of the irradiation period, the mineralization rate started to reduce due to the accumulation of more stable oxidation products and $^{\bullet}OH$ radical recombination. A similar two-step phenol degradation inside a UV/H_2O_2 system using a 24 W UV lamp power was also reported [30]. For the first 15 min, the phenol degradation rate mainly depends on the concentration of H_2O_2 with its k, the order of reaction of phenol and H_2O_2 were 0.035 min^{-1}, 0.205 and 0.490, respectively. While for phase II it was reported as 0.110 min^{-1}, 0.487, 0.169, respectively [30]. Mineralization of Profenofos using UV, Fenton, UV/H_2O_2, $UV/H_2O_2/Fe^{3+}$, and $UV/H_2O_2/Fe^{2+}$ was found to follow pseudo-first order with respect to TOC concentration while the reported values for k ranges from 0.0052 to 0.0973 min^{-1} [31].

3.2 Estimation of activation energy

The effect of reaction temperature, on the rate of OTC mineralization is shown in Fig. 8, for the temperature range of 20–50°C. Similar trends were also reported for the degradation of phenol,

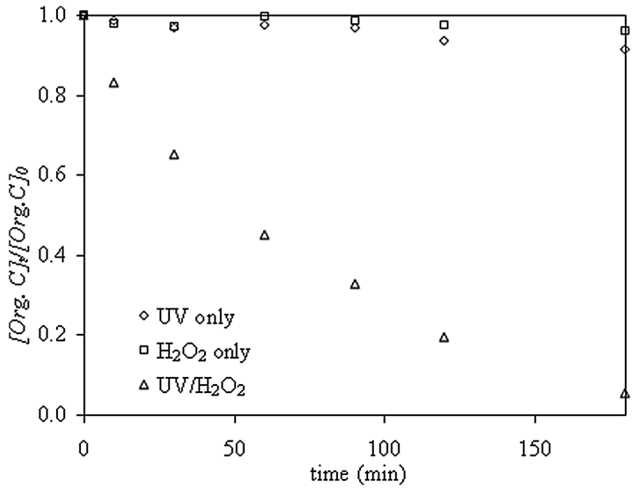

Figure 3. Concentration profile of org. C at 0.116 M of H_2O_2 and at $T = 30°C$ using different mineralization method.

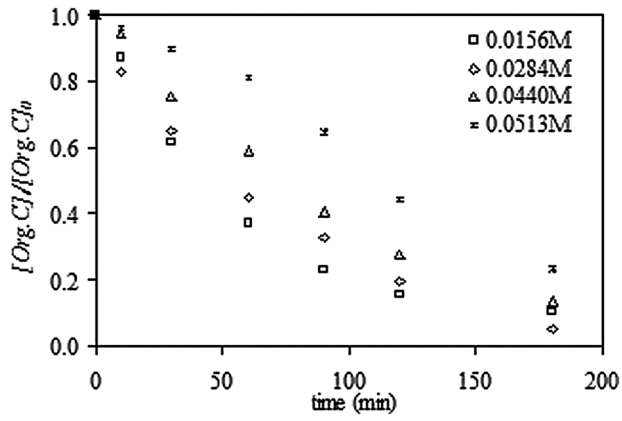

Figure 4. Concentration profile of org.C at 0.116 M of H_2O_2 and at $T = 30°C$ for different concentration of Org. C.

CLEAN Soil Air Water

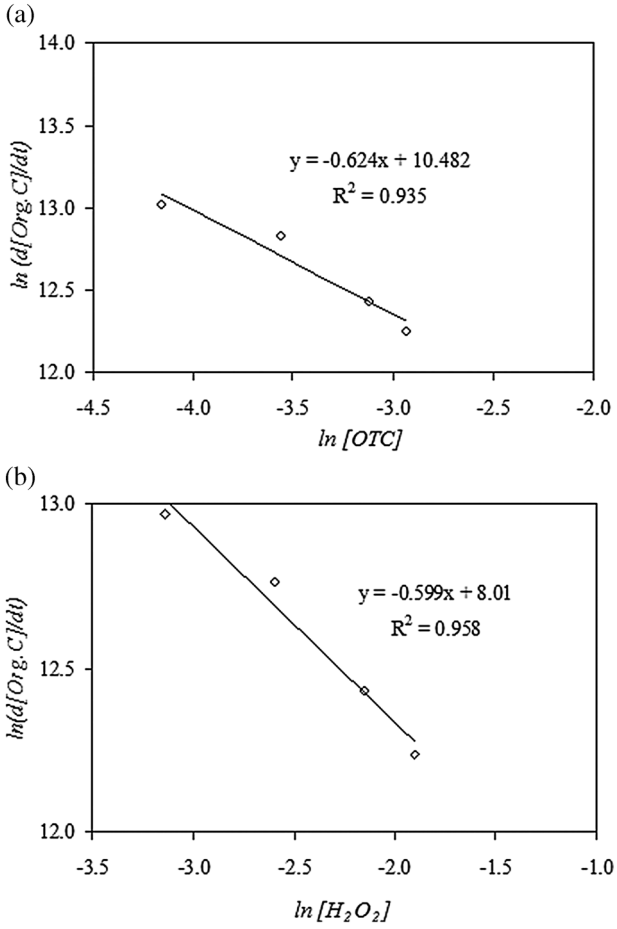

Figure 5. Plot of ln(d[org. C]$_t$/dt) vs. ln([org. C]) for phase I (a) org. C and (b) H_2O_2.

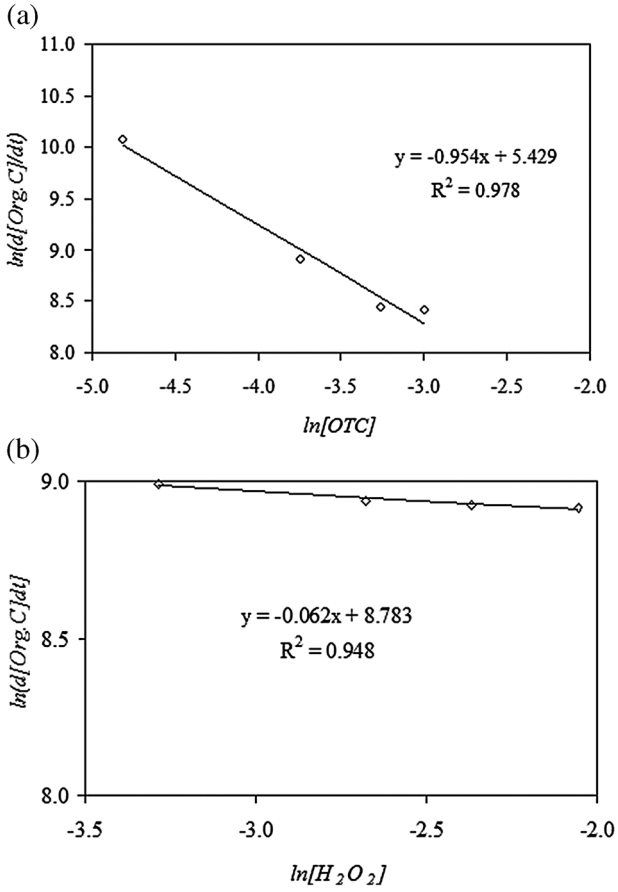

Figure 6. Plot of ln(d[org. C]$_t$/dt) vs. ln([org. H_2O_2]) for phase II (a) org. C and (b) H_2O_2.

4-chlorophenol, 4-nitrophenol, *p*-nitroaniline; OTC hydrolysis and photolysis; oxidation of C. I. food yellow 3 and 4 [22, 32–35]. E_A was calculated using Arrhenius equation:

$$\ln k_{obs} = \ln A - \frac{E_A}{RT} \quad (9)$$

where A is the pre-exponential factor and R the gas constant (8.314 J K^{-1} mol^{-1}). Both E_A and A are the Arrhenius parameters. The differential form of Eq. (9) can be written as:

$$\frac{d(\ln k_{obs})}{dT} = \frac{E_A}{RT^2} \quad (10)$$

Using the plot of ln(−k_{obs}) vs. 1/T, the estimated value of the pre-exponential factor (A) for phase I and phase II of the OTC mineralization are 143.34 and 245.427 s^{-1}, respectively (Fig. 8). The activation energy (E_A) was then derived from the slope of ln(−k_{obs}) vs. 1/T plots, which are 10.236 and 9.913 kJ mol^{-1} for phase I and phase II of the OTC mineralization, respectively. The exponential term of the Arrhenius equation indicates the dependency of kinetic rate constant on temperature [36]. The values of reported activation energies for the degradation of several organic compounds are compared in Tab. 4. Smaller value of E_A was obtained for this present system which indicates lower energy is needed to initiate the reaction. Similar values of activation energy were also reported for the degradation of phenol, 4-nitrophenol, and 4-chlorophenol using UVA/TiO_2 system [32]. It is also possible to estimate rate constant by incorporating hydroxyl radical into the kinetic equation, such as for kinetics of phenol and *p*-nitroaniline degradation. Phenol degradation using a non-catalytic wet air oxidation process and Fenton oxidation of *p*-nitroaniline was found to have higher activation energy values of 77 ± 8 and 53.96 kJ mol^{-1}, respectively [33, 34].

3.3 Thermodynamic studies of OTC mineralization

Thermodynamic properties of OTC mineralization can be explained from the values of Gibbs energy of activation ($\Delta^{\#}G$), enthalpy of

Table 3. Results of differential method plots of OTC mineralization kinetics

Phase I			Phase II		
Org. C (M)	H_2O_2 (M)	k	Org. C (M)	H_2O_2 (M)	k
0.0156	0.116	0.0064	0.0081	0.081	0.0068
0.0284	0.116	0.0069	0.0237	0.094	0.0076
0.0440	0.116	0.0060	0.0381	0.103	0.0076
0.0531	0.116	0.0064	0.0498	0.100	0.0060

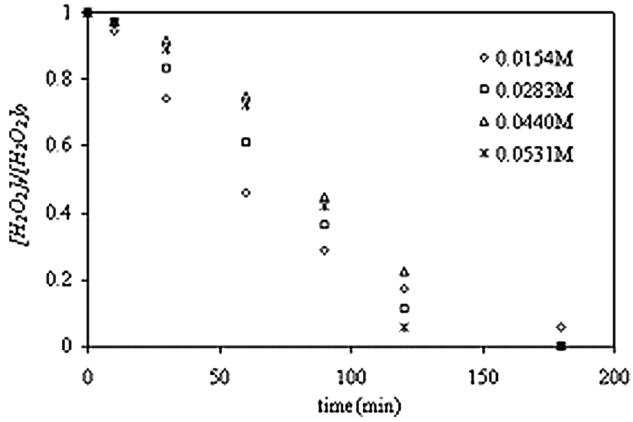

Figure 7. H_2O_2 consumption profile of OTC at 0.116 M H_2O_2 and $T = 30°C$.

activation ($\Delta^{\#}H$), and entropy of activation ($\Delta^{\#}S$) as described below:

$$\Delta^{\#}G = \Delta^{\#}H - T\Delta^{\#}S \tag{11}$$

These parameters are widely used to report experimental reaction rates, especially for organic reactions in solution. For this purpose the following form of Eyring–Polanyi equation was employed [36].

$$k_{obs} = \frac{k_B T}{h} e^{-\Delta^{\#}G/RT} \tag{12}$$

where k_B is the Boltzman constant ($1.380 \times 10^{-23}\,J\,K^{-1}$), T the reaction temperature (K), h the Planck constant ($6.626 \times 10^{-34}\,J\,s^{-1}$), and R is the gas constant ($8.314\,J\,K^{-1}\,mol^{-1}$). The following logarithmic form of the above equation can be used for the estimation of $\Delta^{\#}G$ value.

$$\ln k_{obs} = \ln \frac{k_B T}{h} - \frac{\Delta^{\#}G}{R\,T} \tag{13}$$

Substitution of Eqs. (10), (11), and (12) into the differential form of Eq. (13) results in the following equation:

$$\frac{d(\ln k_{obs})}{dT} = \frac{E_A}{RT^2} = \frac{d}{dT}\left(\ln \frac{k_B T}{h}\right) - \frac{d}{dT}\left(\frac{\Delta^{\#}H}{RT} - \frac{\Delta^{\#}S}{R}\right) \tag{14}$$

With the prior knowledge of E_A, the enthalpy of activation ($\Delta^{\#}H$), could be estimated as follows:

$$\Delta^{\#}H = E_A - RT \tag{15}$$

Using the above equation, the values of $\Delta^{\#}G$, $\Delta^{\#}H$, and $\Delta^{\#}S$ of the OTC mineralization were estimated and are presented in Tab. 5. The Gibbs free energy of activation quantifies the difference between the transition state of reaction and the ground state of the reactants [37]. In transition state, the bonds of the reacting compounds are partially formed and broken. The energy required for bond reorganization is reflected by the higher energy content of the activated complex and corresponds to $\Delta^{\#}H$ [38]. The entropy of activation quantifies the degree of structural organization of the activated complex formation. A reduction of translational, vibrational, and rotational degrees of freedom of the transition state results in negative $\Delta^{\#}S$ [38]. In the present study, the estimated Gibbs free energies and enthalpies of activation are positive whereas the entropies of activation are negative for both phases I and II of the OTC mineralization process. A positive value of $\Delta^{\#}G$ refers to the tendency of transition state of reaction toward the product side is non-spontaneous. These results are in accordance with the fact that no OTC mineralization took place when UV or H_2O_2 alone were being introduced into the system (Fig. 3). A positive value of $\Delta^{\#}G$ was also reported for phenol, 4-chlorophenol, and 4-nitrophenol and C.I. food yellow 3 mineralization, which indicates non-spontaneity of the reaction [32]. For phases I and II, $\Delta^{\#}G$ has the same order with C.I. food yellow 4 [38]. However, the value of $\Delta^{\#}G$ is higher compared to the values obtained in the present study. A positive value for $\Delta^{\#}H$ indicates the energy needed to be supplied to the system in order to achieve the transition energy level which leads to the formation of products. The incorporation of UV/H_2O_2 into the system has supplied energy that overcomes the energy barrier led to OTC mineralization (Fig. 3). A negative value for $\Delta^{\#}S$ can be attributed to the formation of a complex intermediate by OTC and hydroxyl radical, then frequently followed by an entropy reduction through the loss of rotational degrees of freedom of reactant and OTC parent compound during the process [36, 38, 39]. A similar negative value of $\Delta^{\#}S$ was also reported for the thermal isomerization of allyl vinyl ether which in this case lost its rotational degree of freedom by forming

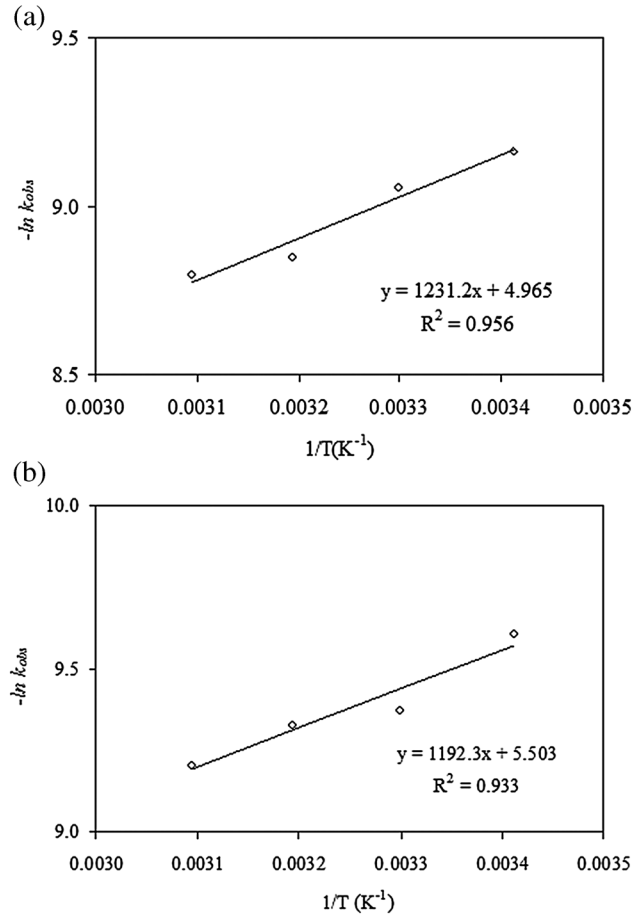

Figure 8. Effect of temperature on the kinetic rate constant (k_{obs}) for (a) phase I and (b) phase II of OTC mineralization.

Table 4. Reported activation energy values for the degradation of different organic compounds under different conditions

Compound	System	E_A (kJ mol^{-1})	Reference
Oxytetracycline degradation	Hydrolysis	88.1 ± 5	[22]
Phenol degradation	UVA/TiO_2	21.44	[32]
4-Chlorophenol degradation	UVA/TiO_2	9.68	[32]
4-Nitrophenol degradation	UVA/TiO_2	18.86	[32]
Phenol	Non-catalytic wet air oxidation	77 ± 8	[33]
p-Nitroaniline degradation	Fenton	53.96	[34]
C.I. food yellow 3 degradation	H_2O_2 oxidation	51	[35]
C.I. food yellow 4 degradation	H_2O_2 oxidation	101	[35]
Oxytetracycline mineralization	UV/H_2O_2	Phase I ($0 \leq t \leq 30$ min): 10.236 Phase II ($30 \leq t \leq 180$ min): 9.913	Present study

Table 5. Thermodynamic parameters of OTC mineralization

T (K)	k (s^{-1})	$\Delta^{\#}G$ (kJ mol^{-1})	$\Delta^{\#}H$ (kJ mol^{-1})	$\Delta^{\#}S$ (J K^{-1} mol^{-1})
Phase I				
293.15	0.00011	49.424	7.799	−141.993
303.15	0.00012	51.460	7.716	−144.299
313.15	0.00014	53.786	7.633	−147.385
323.15	0.00015	55.718	7.550	−149.060
Phase II				
293.15	0.000067	48.339	7.476	−139.395
303.15	0.000085	50.662	7.392	−142.734
313.15	0.000089	52.538	7.309	−144.432
323.15	0.000101	54.628	7.226	−146.686

Table 6. Reported values of thermodynamic parameters for different other organic contaminants

Compound	T (K)	$\Delta^{\#}G$ (kJ mol^{-1})	$\Delta^{\#}H$ (kJ mol^{-1})	$\Delta^{\#}S$ (J K^{-1} mol^{-1})	Reference
Phenol	298.15	86.32	18.97	−0.23	[35]
4-Chlorophenol	298.15	86.26	7.21	−0.27	[35]
4-Nitrophenol	298.15	85.46	16.38	−0.23	[35]
C.I. food yellow 3	298.15	103.00	15.50	+270.00	[38]
C.I. food yellow 4	298.15	54.00	10.30	+140.00	[38]

highly ordered transition state of 4-pentenal [38]. Photodegradation of phenol, 4-chlorophenol and 4-nitrophenol also have negative $\Delta^{\#}S$ values [32]. Table 6 shows the comparison of the reported values of $\Delta^{\#}G$, $\Delta^{\#}H$, and $\Delta^{\#}S$ for the mineralization of different compounds using different processes.

4 Conclusions

Based on the org. C of OTC and H_2O_2 concentration profile, kinetic and thermodynamic parameters of OTC mineralization using a UV/H_2O_2 system at its optimum pH were evaluated. The experimental data were analyzed for pseudo zero-th, first, and second order to find the order of reaction of OTC mineralization. Differential method was also used for obtaining the order of reaction. Based on the analysis and also the mechanistic aspects provided by each of the kinetic models, the kinetic equation of OTC mineralization was obtained based on the differential method rather than pseudo order plot. Based on the present kinetic analysis, it can be concluded that the reaction follows the pseudo first order kinetics, for both the regimes with different k values, which include the concentration of both OTC as well as H_2O_2. The temperature dependency of OTC mineralization was studied by using the Arrhenius equation and low value of E_A was obtained. The values of the Arrhenius constant (A) show the positive effect of temperature on the reaction. The value of the thermodynamic parameters of the OTC mineralization, such as $\Delta^{\#}G$, $\Delta^{\#}H$, and $\Delta^{\#}S$ were also determined. In this study, positive values of $\Delta^{\#}G$ and $\Delta^{\#}H$ and negative values of $\Delta^{\#}S$ were obtained for phases I and II of OTC mineralization, indicating the non-spontaneity of the reaction. The present results will certainly be useful for the design and scale up of the OTC mineralization process toward commercial/large scale process.

The authors have declared no conflict of interest.

References

[1] C. G. Daughton, T. A. Ternes, Pharmaceuticals and Personal Care Products in the Environment: Agents of Subtle Change?, *Environ. Health Perspect.* **1999**, *107*, 907–942.

[2] J. B. Ellis, Pharmaceutical and Personal Care Products (PPCPs) in Urban Receiving Water, *Environ. Pollut.* **2006**, *144*, 184–189.

[3] A. Karci, I. A. Balcioglu, Investigation of the Tetracycline, Sulfonamide, and Fluoroquinolone Antimicrobial Compounds in Animal

Manure and Agricultural Soils in Turkey, *Sci. Total Environ.* **2009**, *407*, 4652–4654.

[4] M. Edwards, E. Topp, C. D. Metcalfe, H. Li, N. Gottschall, P. Bolton, W. Curnoe, et al., Pharmaceutical and Personal Care Products in Tile Drainage Following Surface Spreading and Injection of Dewatered Municipal Biosolids to an Agricultural Field, *Sci. Total Environ.* **2010**, *407*, 4220–4230.

[5] D. Li, M. Yang, J. Hu, Y. Zhang, H. Chang, F. Jin, Determination of Penicillin G and Its Degradation Products in a Penicillin Production Wastewater Treatment Plant and the Receiving River, *Water Res.* **2008**, *42*, 307–317.

[6] W. Xu, G. Zhang, X. Li, S. Zou, P. Li, Z. Hu, J. Li, Occurrence and Elimination of Antibiotics at Four Sewage Treatment Plants in the Pearl River Delta (PRD), South China, *Water Res.* **2007**, *41*, 4526–4534.

[7] K. Kümmerer, Antibiotics in the Aquatic Environment, *Chemosphere* **2009**, *75*, 417–434.

[8] M. Klavarioti, D. Mantzavinos, D. Kassinos, Removal of Residual Pharmaceuticals from Aqueous Systems by Advanced Oxidation Processes, *Environ. Int.* **2009**, *35*, 402–417.

[9] F. Baquero, J. L. Martinez, R. Canton, Antibiotics and Antibiotic Resistance in Water Environments, *Curr. Opin. Biotechnol.* **2008**, *19*, 260–265.

[10] V. J. L. Martinez, Environmental Pollution by Antibiotics and by Antibiotic Resistance Determinants, *Environ. Pollut.* **2009**, *157*, 2893–2902.

[11] C. Garafalo, C. Viragnoli, G. Zandri, L. Aquilanti, D. Bordoni, A. Osimani, F. Clementi, et al., Direct Detection of Antibiotics Resistance Genes in Specimens of Chicken and Pork Meat, *Int. J. Food Microbiol.* **2007**, *113*, 75–83.

[12] A. Gulkowska, H. W. Leung, M. K. So, S. Taniyasu, N. Yamashita, L. W. Y. Yeung, B. J. Richardson, et al., Removal of Antibiotics from Wastewater by Sewage Treatment Facilities in Hongkong and Shenzhen, China, *Water Res.* **2008**, *42*, 395–403.

[13] F. C. Cabello, Heavy Use of Prophylactic Antibiotics in Aquaculture: A Growing Problem for Human and Animal Health and for the Environment, *Environ. Microbiol.* **2006**, *8*, 1137–1144.

[14] M. O. Uslu, I. A. Balcioglu, Comparison of the Ozonation and Fenton Process Performance for the Treatment of Antibiotic Containing Manure, *Sci. Total Environ.* **2009**, *407*, 3450–3458.

[15] A. J. Bauger, J. Hensen, P. H. Krogh, Effects of Antibiotics Oxytetracycline and Tylosin on Soil Fauna, *Chemosphere* **2000**, *40*, 751–757.

[16] Y. Wang, L. Wang, F. Li, J. Liang, Y. Li, J. Dai, T. C. Loh, et al., Effects of Oxytetracycline and Sulfachloropyridazine Residues on the Reductive Activity of *Shewanella decoloratis* S12, *J. Agric. Food Chem.* **2009**, *57*, 5878–5883.

[17] O. A. Arikan, C. Rice, E. Codling, Occurrence of Antibiotics and Hormones in a Major Agricultural Watershed, *Desalination* **2008**, *226*, 121–133.

[18] I. R. Bautiz, R. F. P. Nogueira, Degradation of Tetracycline by Photo-Fenton Process-solar Irradiation and Matrix Effects, *J. Photochem. Photobiol., A* **2007**, *187*, 33–39.

[19] K. Li, A. Yediler, M. Yang, S. Schulte-Hostede, M. H. Wong, Ozonation of Oxytetrcycline and Toxicological Assessment of Its Oxidation By-products, *Chemosphere* **2008**, *72*, 472–478.

[20] Y. Chen, C. Hu, J. Qu, M. Yang, Photodegradation of Tetracycline and Formation of Reactive Oxygen Species in Aqueous Tetracycline under Simulate Sunlight Irradiation, *J. Photochem. Photobiol., A* **2008**, *197*, 81–87.

[21] S. Jiao, S. Zheng, D. Yin, L. Wang, L. Chen, Aqueous Oxytetracycline Degradation and the Toxicity Change of Degradation Compounds in Photoirradiation Process, *J. Environ. Sci.* **2008**, *20*, 806–813.

[22] R. Xuan, L. Arisi, Q. Wang, S. R. Yates, K. C. Biswas, Hydrolysis and Photolysis of Oxytetracycline in Aqueous Solution, *J. Environ. Sci. Health, Part B* **2010**, *45*, 73–81.

[23] C. Zhao, H. Deng, Y. Li, Z. Liu, Photodegradation of Oxytetracycline in Aqueous by 5A and 13X Loaded with TiO_2 under UV Irradiation, *J. Hazard. Mater.* **2010**, *176*, 884–892.

[24] X. Wen, Y. Jia, J. Li, Enzymatic Degradation of Tetracycline and Oxytetracycline by Crude Manganese Peroxidase Prepared from *Phanerochaete chrysosporium*, *J. Hazard. Mater.* **2010**, *177*, 924–928.

[25] F. Yuan, C. Hu, X. Hu, D. Wei, Y. Chen, J. Qu, Photodegradation and Toxicity Changes of Antibiotics in UV and UV/H_2O_2 Process, *J. Hazard. Mater.* **2011**, *185*, 1256–1263.

[26] N. K. Shammas, L. K. Wang, in *Handbook of Advanced Industrial and Hazardous Waste Treatment* (Eds.: L. K. Wang, N. K. Shammas, Y. T. Hung), CRC Press, Boca Raton, FL **2009**, p. 407.

[27] A. U. Rahmah, S. Harimurti, A. A. Omar, T. Murugesan, Optimization of Oxytetracycline Mineralization Using Box-Behnken Experimental Design inside a UV/H_2O_2 System, *J. Appl. Sci.* **2012**, *12*, 1154–1159.

[28] T. Oppenlander, *Photochemical and Purification of Water and Air*, Wiley-VCH Verlag, Weinheim, Germany **2003**, p. 190.

[29] M. I. Stefan, A. R. Hoy, J. R. Bolton, Kinetics and Mechanism of Degradation and Mineralization of Acetone in Dilute Aqueous Solution Sensitized by the UV Photolysis of Hydrogen Peroxide, *Environ. Sci. Technol.* **1996**, *30*, 2382–2390.

[30] A. K. De, S. Bhattacharjee, B. K. Dutta, Kinetics of Phenol Photooxidation by Hydrogen Peroxide and Ultraviolet Radiation, *Ind. Eng. Chem. Res.* **1997**, *36*, 3607–3612.

[31] M. I. Badawy, M. Y. Ghaly, T. A. Gad-Allah, Advanced Oxidation Processes for the Removal of Organo-phosphorus Pesticides from Wastewater, *Desalination* **2006**, *194*, 166–175.

[32] K. Naeem, P. Weiqian, F. Ouyang, Thermodynamic Parameters of Activation for Photodegradation of Phenolics, *Chem. Eng. J.* **2010**, *156*, 505–509.

[33] S. Lefèvre, O. Boutin, J. H. Ferasse, L. Malleret, R. Faucherand, A. Viand, Thermodynamic and Kinetic Study of Phenol Degradation by a Non-catalytic Wet Oxidation, *Chemosphere* **2011**, *84*, 1208–1215.

[34] J.-H. Sun, S.-P. Sun, M.-H. Fan, H.-Q. Guo, L.-P. Qiao, R.-X. Sun, A Kinetic Study on the Degradation of *p*-Nitroaniline by Fenton Oxidation Process, *J. Hazard. Mater.* **2007**, *148*, 172–177.

[35] C. T. Fragoso, R. Battisti, C. Miranda, P. C. de Jessus, Kinetic Degradation of C.I. Food Yellow 3 and C. I. Food Yellow 4 Azo Dyes by the Oxidation with Hydrogen Peroxide, *J. Mol. Catal. A: Chem.* **2009**, *301*, 93–97.

[36] P. Atkins, J. de Paula, *Physical Chemistry*, 8th Ed., W. Freeman, New York **2006**, pp. 807–809.

[37] IUPAC, *Compendium of Chemical Terminology*, 2nd Ed. (the "Gold Book") (Eds.: A. D. McNaught, A. Wilkinson), Blackwell, Oxford **1997**.

[38] F. A. Carey, R. J. Gundberg, *Advanced Organic Chemistry, Part A: Structure and Mechanism*, Springer, New York, USA **2007**, p. 203.

[39] M. Graber, M. Bousquet-Dubouch, N. Sousa, S. Lamare, M. Legoy, Water Plays a Different Role on Activation Thermodynamic Parameters of Alcoholysis Reaction Catalyzed by Lipase in Gaseous and Organic Media, *Biochim. Biophys. Acta* **2002**, *1645*, 56–62.